gions of cosmids was finished for only one clone), and all ambiguities in the sequence were resolved before the sequence of a clone was considered finished. The finished sequences were compared with the public sequence databases for protein and nucleic acid homologies [SWISSPROT (release 28.0), PIR (release 40.0), and GENPEPT (release 82.0)], with BLASTX (for protein similarities) and BLASTN (for nucleotide similarities) (*18*) and searched for tRNAs with TRNASCAN [G. Fichant and C. Burks, *J. Mol. Biol.* **220**, 659 (1991)]. The sequence of each cosmid was also compared to the yeast sequences in GenBank, and discrepancies were examined in our sequence and corrected when possible (however, we judged that very few of these differences were due to mistakes in our sequence). The finished sequences were assembled and interactively annotated with AScDB, a version of the *Caenorhabditis elegans* database program ACeDB (R. Durbin and J.-T. Mieg, unpublished results) modified (by E. Sonhammer and R. Durbin and L. Hillier) for use with yeast data. At this point, any potential frameshift errors were recognized, and the appropriate regions were resequenced to resolve the problems. Portions of the chromosome (usually individual cosmids) were submitted to GenBank, as shown in Fig. 1 (entry names and accession numbers are also listed in Table 1). Only a small number of overlapping bases were included in each database entry to facilitate joining of the sequences or to keep a gene intact. In addition, the entire (nonoverlapping) 562,638 bp of DNA that comprise chromosome VIII are available via anonymous file transfer protocol (ftp) (genome-ftp-.stanford.edu in the directory: /pub/yeast/genome_seq/chrVIII; ncbi.nlm.nih.gov in the directory: /repository/yeast/CHVIII). All ORFs containing at least 100 codons (including the ATG and translation termination codons) were identified. This analysis was done in batch with two scripts (ASCPREP1 and ASCPREP2; L. Hillier, unpublished results) that prepare the sequence and the database search results for entry into AScDB, which was used interactively to annotate the sequence. Genes were chosen with the help of the GENEFINDER program (P. Green and L. Hillier, unpublished results) modified (by L. Hillier, E. Sonhammer, and R. Durbin) for use with *S. cerevisiae*. All genes larger than 100 codons were annotated, except in the case of overlapping genes, where the longest gene or the gene that had homology to another gene was chosen. The first ATG codon in an ORF was always chosen as the beginning of the gene. Splice sites were used as necessary and when possible to construct a gene; a TACTAAC box 5 to 134 bases upstream of the 3′ splice site [B. C. Rymond and M. Rosbash, in *The Molecular and Cellular Biology of the Yeast Saccharomyces*, E. Jones, J. Pringle, J. Broach, Eds. (Cold Spring Harbor Laboratory Press, Cold Spring Harbor, NY, 1992), vol. 2, pp. 143–192] was demanded in each case. We sought delta (δ), sigma (σ), and tau (τ) elements by comparing the sequence using BLASTN and FASTA against a representative member of each element.

4. L. Riles *et al.*, *Genetics* **134**, 81 (1993); L. Riles and M. Olson, unpublished results.
5. This is a conservative accuracy estimate based on our analysis of the yeast sequence as well as of the *C. elegans* sequence that has been determined in our sequencing center. We identified mistakes in the yeast sequence by comparing our sequence to sequences already in GenBank and by recognizing apparent frameshift errors. In 425 kb of yeast sequence checked in this way, 24 potential errors were identified (two by comparison to sequences in GenBank and 22 by recognition of apparent frameshifts)—approximately one error in 17 kb (most of these errors were corrected). An independent comparison of 17,208 bp of *C. elegans* sequence to an independently determined sequence already in GenBank revealed one error (L. Hillier, unpublished results), corroborating our estimate of approximately one mistake per 17 kb.
6. B. Dujon, personal communication.
7. M. V. Olson, in *The Molecular and Cellular Biology of the Yeast Saccharomyces*, E. Jones, J. Pringle, J. Broach, Eds. (Cold Spring Harbor Laboratory Press, Cold Spring Harbor, NY, 1991), vol. 1, pp. 1–40.
8. D. F. Voytas and J. D. Boeke, *Nature* **358**, 717 (1992).
9. R. R. Butt and D. J. Ecker, *Microbiol. Rev.* **51**, 351 (1987).
10. The "top" strand refers to the strand with polarity 5′ to 3′ (left to right) of the chromosome as oriented (according to convention) on the genetic map of R. K. Mortimer *et al.* [*Yeast* **8**, 817 (1992)].
11. The distribution of G+C content for chromosome VIII was found to be statistically different ($\alpha > 0.01$) from that of a random sequence with the same nucleotide content. Further, the analysis confirmed that the three major peaks in the chromosome VIII G+C content plots are significantly different from that of the random sequence (three to four times as many standard deviations from the mean as peaks in the random sequence) (L. Hillier and G. Marth, in preparation).
12. P. M. Sharp and A. T. Lloyd, *Nucleic Acids Res.* **21**, 179 (1993).
13. H. Bussey, personal communication.
14. H. Y. Steensma, P. De Jonge, A. Kaptein, D. B. Kaback, *Curr. Genet.* **16**, 131 (1989).
15. D. Lalo, S. Stettler, S. Mariotte, P. Slonimski, P. Thuriaux, *C. R. Acad. Sci. Paris* **316**, 367 (1993).
16. E. J. Louis, E. S. Naumova, A. Lee, G. Naumov, J. E. Haber, *Yeast* **10**, 271 (1994).
17. These comparisons were performed at the National Center for Biotechnology Information with the BLAST network service.
18. S. F. Altschul, W. Gish, W. Miller, E. W. Myers, D. J. Lipman, *J. Mol. Biol.* **215**, 403 (1990).
19. S. Henikoff and J. G. Henikoff, *Genomics* **19**, 97 (1994).
20. We thank H. Bussey for providing the sequence of yeast chromosome I and E. Sonhammer and R. Durbin for modifing GENEFINDER for use with yeast data. Supported by a grant from the NIH National Center for Human Genome Research. E.J.L. received support from the Wellcome Trust.

16 August 1994; accepted 1 September 1994

Specific Cleavage of Model Recombination and Repair Intermediates by the Yeast Rad1-Rad10 DNA Endonuclease

A. Jane Bardwell,*† Lee Bardwell,*‡ Alan E. Tomkinson, Errol C. Friedberg§

The *RAD1* and *RAD10* genes of *Saccharomyces cerevisiae* are required for both nucleotide excision repair and certain mitotic recombination events. Here, model recombination and repair intermediates were used to show that Rad1-Rad10–mediated cleavage occurs at duplex–single-strand junctions. Moreover, cleavage occurs only on the strand containing the 3′ single-stranded tail. Thus, both biochemical and genetic evidence indicate a role for the Rad1-Rad10 complex in the cleavage of specific recombination intermediates. Furthermore, these data suggest that Rad1-Rad10 endonuclease incises DNA 5′ to damaged bases during nucleotide excision repair.

The *S. cerevisiae RAD1* and *RAD10* genes are involved in both nucleotide excision repair (*1*) and mitotic recombination (*2–9*). *RAD1* is the probable homolog of the human *XPF* (*ERCC4*) gene, which is defective in the cancer-prone disease xeroderma pigmentosum (*10*, *11*); *RAD10* is homologous to human *ERCC1* (*12*). Rad1 and Rad10 proteins form a stable complex (*13*, *14*) that catalyzes the endonucleolytic degradation of single-stranded bacteriophage DNA but is inactive on linear duplex DNA (*15*, *16*). Here we demonstrate that rather than exhibiting a generalized single-strand DNA endonuclease activity as previously indicated (*15*, *16*), Rad1-Rad10 protein is a duplex–3′ single-strand junction-specific endonuclease. The characterization of this structure-specific activity greatly clarifies the role of Rad1-Rad10 protein in recombination and DNA repair.

Single-stranded, duplex, or partial duplex model DNA substrates were generated from synthetic oligonucleotides 18 to 50 nucleotides in length (Table 1). Rad1-Rad10 endonuclease did not degrade a single-stranded 49-nucleotide oligomer (S1 in Table 1 and Fig. 1, A and B) or a 49–base pair (bp) duplex structure (D in Table 1 and Fig. 2, A and B). However, when S1 was annealed to shorter complementary oligonucleotides, partial duplex molecules containing 3′ single-stranded tails (TD1 and TD2 in Table 1) were cleaved by the enzyme (Fig. 1A), whereas substrate TD3 (Table 1) containing a 5′ single-stranded tail was not (Fig. 1A). In a similar manner, substrate S3 (Table 1) was not cleaved as a single-stranded oligonucleotide (Fig. 2B), nor as a partial duplex derivative with a 5′ single-stranded tail (TD4 in Table 1 and Fig. 1A). A partial duplex derivative with a 3′ tail was cleaved (TD5 in Table 1 and Fig. 1A).

Analyses with denaturing gels demon-

A. J. Bardwell, L. Bardwell, E. C. Friedberg, Laboratory of Molecular Pathology, The University of Texas Southwestern Medical Center at Dallas, Dallas, TX 75235, USA.
A. E. Tomkinson, Institute for Biotechnology, Center for Molecular Medicine, The University of Texas Health Science Center at San Antonio, San Antonio, TX 78245, USA.

*These authors contributed equally to this study.
†Present address: Genelabs Technologies Inc., 505 Penobscot Drive, Redwood City, CA 94063, USA.
‡Present address: Department of Molecular and Cell Biology, University of California at Berkeley, Berkeley, CA 94720, USA.
§To whom correspondence should be addressed.

strated that incision of the 3′ tailed substrate TD1 occurred exclusively within the duplex region of strand S1, primarily at positions located 2, 3, and 4 nt 5′ to the duplex–single-strand junction (Fig. 1B). Strand S3 in the 3′ tailed substrate TD5 was similarly cut primarily at positions 2, 3, and 5 nucleotides 5′ to the duplex–single-strand junction (Fig. 1B). This heterogeneity of the cleavage position presumably reflects breathing of the duplex–single-strand junctions during the incubations. Cleavage was not observed in the single-stranded region of any substrate (Fig. 1B), nor on those strands (S11 to S15 in TD1 to TD5, respectively, in Table 1) that were strictly in duplex regions (*17*).

A Y-shaped partial duplex structure with a 31-bp duplex region and 19- and 18-nucleotide single-stranded tails (PD A and PD B in Table 1) was cleaved by Rad1-Rad10 endonuclease in a concentration-dependent manner (Fig. 2A). The reaction products observed on nondenaturing gels were identical regardless of whether strand S1 or S3 was 5′ end-labeled (Fig. 2A), which indicates that both 5′ ends were retained and suggests that the 3′ single-stranded tail was removed in each case. Denaturing gel electrophoresis confirmed that cleavage of the Y substrate occurred in strand S1 within the duplex region, primarily at a position 2 nucleotides 5′ to the duplex–single-strand junction (Fig. 2B). Incision was not observed in the opposite strand (S3) (Fig. 2B).

In summary, of the various substrates examined, Rad1-Rad10–catalyzed cleavage occurred only in the duplex region at duplex–single-strand junctions and had a preference for nucleotide position +2 relative to the junction. Nicking occurred exclusively on strands with 3′ tails (Fig. 3A). Purified Rad1-Rad10 complex has no exonuclease activity (*15*, *16*). Previous observations that this complex cleaves single-stranded bacteriophage DNA but not double-stranded DNA suggested that Rad1-Rad10 protein was a single-stranded endonuclease (*15*, *16*). The present results indicate that the enzyme is rather a duplex–3′ single-strand junction-specific endonuclease. Hence, the observed cleavage of M13 single-stranded DNA (*15*, *16*) may occur at duplex–single-strand junctions of stem-loop structures typically present in single-stranded bacteriophage DNA.

The junction-specific endonuclease activity of Rad1-Rad10 protein provides an

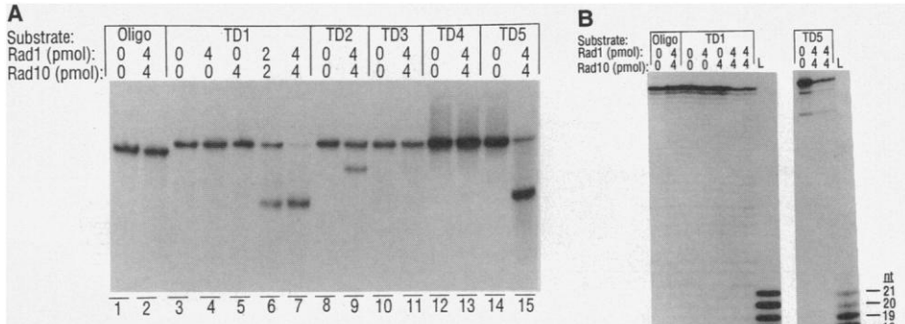

Fig. 1. Rad1-Rad10 endonuclease specifically cleaves 3′ tails. (**A**) Native 15% polyacrylamide gel autoradiogram showing model substrates and cleavage products. Lanes 1 and 2, single-stranded oligo (S1); lanes 3 to 7, 3′-tailed substrate (TD1); lanes 8 and 9, 3′-tailed substrate (TD2); lanes 10 and 11, 5′-tailed substrate (TD3); lanes 12 and 13, 5′-tailed substrate (TD4); and lanes 14 and 15, 3′-tailed substrate (TD5) (Table 1). Substrates were incubated with no protein added (lanes 1, 3, 8, 10, 12, and 14), with 4 pmol of Rad1 protein (lane 4), with 4 pmol of Rad10 protein (lane 5), with 2 pmol each of Rad1 and Rad10 proteins (lane 6), or with 4 pmol each of Rad1 and Rad10 proteins (lanes 7, 9, 11, 13, and 15) (*28*). The percent of substrate cleaved (determined with a Molecular Dynamics Phosphoimager) was 43%, 83%, 36%, and 83% in lanes 6, 7, 9, and 15, respectively. (**B**) Denaturing 10% polyacrylamide gel autoradiogram of reactions parallel to those shown in (A). Lanes 1 and 2, oligonucleotide S1; lanes 3 to 7, substrate TD1; and lanes 9 to 11, substrate TD5. Lanes 8 and 12 contain a 17- to 21-nucleotide ladder (L; positions indicated on the right). Rad1-Rad10 cleavage products are in lanes 6 and 7 (50% of substrate cleaved) and 10 and 11 (76% cleaved). The lower percentage of substrate cleavage as compared to that in (A) is due to partial loss of enzyme activity during storage.

Table 1. Model substrates used in this study. An asterisk indicates that the strand was 5′ ^{32}P end-labeled by T4 polynucleotide kinase. The nonhomologous region of the Y-shaped partial duplex substrate is underlined; nt, nucleotides.

Name	Strands	Sequence	Length (nt)
S1	S1	*5′-CACGCTACCGAATTCTGACTTGCTAGGACATCTTTGCCCACGTTGACCC-3′	49
D	S1	*5′-CACGCTACCGAATTCTGACTTGCTAGGACATCTTTGCCCACGTTGACCC-3′	49
	S2	3′-GTGCGATGGCTTAAGACTGAACGATCCTGTAGAAACGGGTGCAACTGGG-5′	49
TD1	S1	*5′-CACGCTACCGAATTCTGACTTGCTAGGACATCTTTGCCCACGTTGACCC-3′	49
	S11	3′-GTGCGATGGCTTAAGACTG-5′	19
TD2	S1	*5′-CACGCTACCGAATTCTGACTTGCTAGGACATCTTTGCCCACGTTGACCC-3′	49
	S12	3′-GTGCGATGGCTTAAGACTGAACGATCCTGTA-5′	31
TD3	S1	*5′-CACGCTACCGAATTCTGACTTGCTAGGACATCTTTGCCCACGTTGACCC-3′	49
	S13	3′-GAAACGGGTGCAACTGGG-5′	18
S3	S3	*5′-TCGATAGTCTCTAGATAGCATGTCCTAGCAAGTCAGAATTCGGTAGCGTG-3′	50
TD4	S3	*5′-TCGATAGTCTCTAGATAGCATGTCCTAGCAAGTCAGAATTCGGTAGCGTG-3′	50
	S14	3′-CAGTCTTAAGCCATCGCAC-5′	19
TD5	S3	*5′-TCGATAGTCTCTAGATAGCATGTCCTAGCAAGTCAGAATTCGGTAGCGTG-3′	50
	S15	3′-AGCTATCAGAGATCTATCG-5′	19
PD A	S1	*5′-CACGCTACCGAATTCTGACTTGCTAGGACATCTTTGCCCACGTTGACCC-3′	49
	S3	3′-GTGCGATGGCTTAAGACTGAACGATCCTGTACGATAGATCTCTGATAGCT-5′	50
PD B	S1	5′-CACGCTACCGAATTCTGACTTGCTAGGACATCTTTGCCCACGTTGACCC-3′	49
	S3	3′-GTGCGATGGCTTAAGACTGAACGATCCTGTACGATAGATCTCTGATAGCT-5′*	50
TD6	S21	5′-CACGCTACCGAATTCTGACTTGCTAGGAC-3′	29
	S3	3′-GTGCGATGGCTTAAGACTGAACGATCCTGTACGATAGATCTCTGATAGCT-5′	50

explanation for its role in recombination and in the incision step of nucleotide excision repair (NER). In NER, dual incisions are believed to generate an oligonucleotide fragment containing the damage and flanking undamaged bases (*18*). A multiprotein DNA damage-recognition complex containing the Rad3 and Ssl2 helicases (*19*–*21*) may unwind a localized region around a damaged base, thereby generating a duplex–single-strand junction on either side of the damage (Fig. 3B). The Rad1-Rad10 endonuclease may recognize the duplex–3′ single-strand junction 5′ to the damaged base and catalyze endonucleolytic cleavage at that site (Fig. 3B) (*22*). A second endonuclease such as the *RAD2* gene product (*23*) may incise the DNA 3′ to the damage. Indeed, Rad2 protein may also be a duplex–single-strand junction-specific endonuclease but with 5′ polarity (*24*, *25*). This model is not predicated on a particular order of incision with respect to the Rad1-Rad10 and Rad2 endonucleases.

During mitotic recombination between repeated sequences, the *RAD1* gene product is required to remove short regions of nonhomologous DNA from 3′ recombining ends (*8*). Such nonhomology results when an initiating double-strand break occurs in a unique sequence between the repeats. During processing of the break by either single-strand annealing (SSA) (*26*, *27*) (Fig. 3C) or gap repair (*17*), the 3′ ends of the break become single-stranded. This leads to the formation of a duplex–3′ single-strand junction containing the 3′ region of nonhomology during the annealing step of SSA, or the strand invasion step of gap repair (*8*). This junction may constitute a substrate for Rad1-Rad10 endonuclease (Fig. 3C).

In both the NER and SSA models shown, extension by a DNA polymerase is presumed to follow the Rad1-Rad10–mediated incision step. For determination of whether Rad1-Rad10 reaction products provide suitable primer-templates for DNA polymerase, the partial duplex Y substrate (S1 annealed to S3) was incubated with Rad1-Rad10 enzyme and with 3′ exonuclease-free T7 DNA polymerase (Fig. 4). This molecule alone did not provide a suitable substrate for the polymerase (Fig. 4), whereas the control substrate TD6 (Table 1 and Fig. 4) did. Consistent with the mode of cleavage of the partial duplex Y substrate (Figs. 2 and 3), Rad1-Rad10 endonuclease

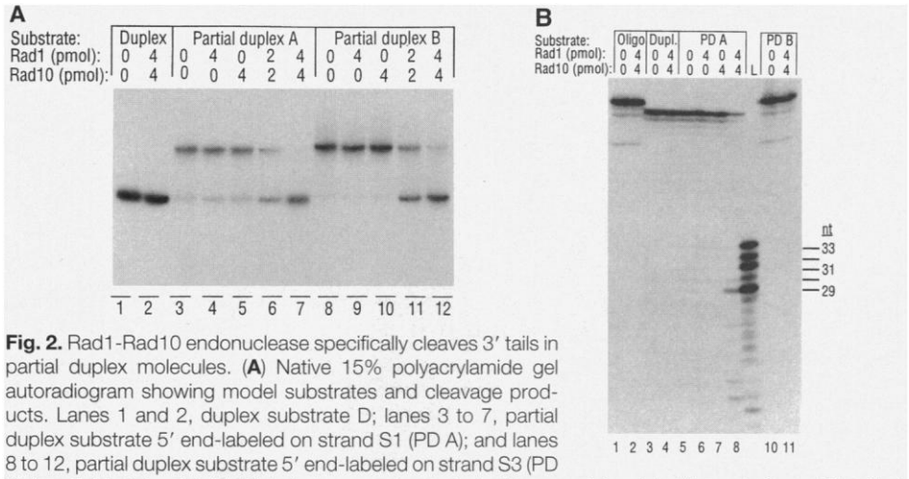

Fig. 2. Rad1-Rad10 endonuclease specifically cleaves 3′ tails in partial duplex molecules. (**A**) Native 15% polyacrylamide gel autoradiogram showing model substrates and cleavage products. Lanes 1 and 2, duplex substrate D; lanes 3 to 7, partial duplex substrate 5′ end-labeled on strand S1 (PD A); and lanes 8 to 12, partial duplex substrate 5′ end-labeled on strand S3 (PD B) (see Table 1 for details). Substrates were incubated with no protein added (lanes 1, 3, and 8), with 4 pmol of Rad1 protein (lanes 4 and 9), with 4 pmol of Rad10 protein (lanes 5 and 10), with 2 pmol each of Rad1 and Rad10 proteins (lanes 6 and 11), or with 4 pmol each of Rad1 and Rad10 proteins (lanes 2, 7, and 12). The percent of substrate cleaved was 55%, 91%, 49%, and 76% in lanes 6, 7, 11, and 12, respectively. The faint lower bands seen in lanes 3 to 5 and lanes 8 to 10 are small amounts of labeled S1 and S3, respectively, which were not annealed into the PD A and PD B structures. A single-stranded 50-nucleotide oligomer has a similar electrophoretic mobility to those of the PD reaction products in a native 15% polyacrylamide gel. (**B**) Denaturing 10% polyacrylamide gel autoradiogram of reactions parallel to those shown in (A). Lanes 1 and 2, oligonucleotide S3; lanes 3 and 4, duplex substrate D; lanes 5 to 8, PD A; and lanes 10 and 11, PD B. Lane 9, 29- to 33-nucleotide ladder (L; positions indicated on the right). Rad1-Rad10 cleavage products are in lane 8 (54% of substrate cleaved).

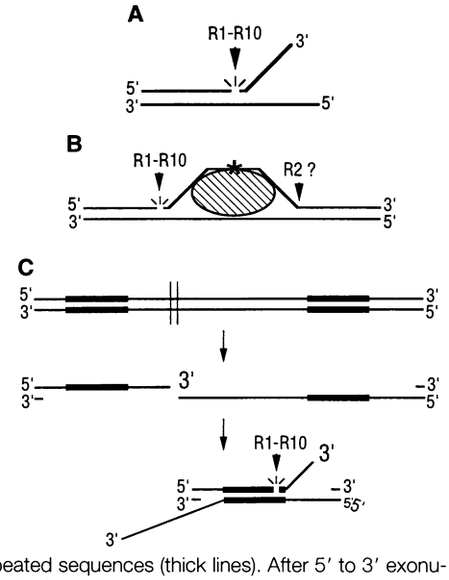

Fig. 3. (**A**) Duplex–3′ single-strand junction-specific endonuclease activity of Rad1-Rad10 enzyme. The endonuclease is shown cleaving within the duplex region of a Y-shaped partial duplex molecule, 2 to 5 nucleotides 5′ to the duplex–single-strand junction. (**B**) Suggested role of this endonuclease activity in the incision step of nucleotide excision repair. The model postulates that the interaction of a multiprotein nucleotide excision repair complex (hatched oval) with damaged DNA results in the generation of duplex–3′ single-strand and duplex–5′ single-strand junctions flanking the site of base damage (shown as an asterisk). The duplex–3′ single-strand junction may be recognized as a specific substrate by the Rad1-Rad10 endonuclease and the duplex–5′ single-strand junction may be recognized by the Rad2 endonuclease (*23*, *24*), a product of the *RAD2* gene, which is known to be involved in nucleotide excision repair (*1*). (**C**) Postulated role of the Rad1-Rad10 endonuclease in the single-strand annealing model of mitotic recombination between repeated sequences. Recombination is initiated by the introduction of a double-strand break (double vertical lines) between two repeated sequences (thick lines). After 5′ to 3′ exonucleolytic degradation from the 5′ ends of the break, the homologous repeats become single-stranded and can anneal. This results in the formation of a duplex–3′ single-strand junction with a short nonhomologous tail (upper strand in the figure). This junction is expected to be a substrate for the Rad1-Rad10 endonuclease. The longer 3′ tail comprising most of the intervening sequence between the repeats (lower strand in the figure) may be much longer and is apparently processed in a different manner (*8*).

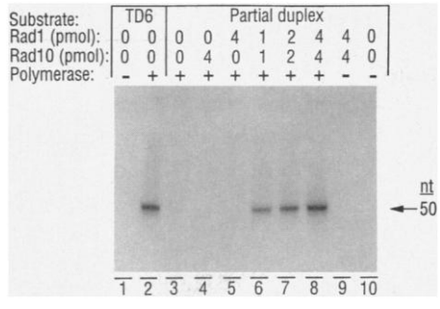

Fig. 4. Rad1-Rad10 cleavage products can be extended by DNA polymerase. The unlabeled partial duplex substrate (strands S1 + S3) or substrate TD6 (Table 1) were incubated with the indicated amounts of Rad1 or Rad10 proteins, or both, for 30 min under conditions described in Fig. 1. ^{32}P deoxyribonucleotide triphosphates were then added for a further 5 min either with (lanes 2 to 8) or without (lanes 1, 9, and 10) T7 3′ exonuclease-free DNA polymerase (Sequenase 2.0; U.S. Biochemical Corp.). Reactions were stopped, deproteinized, and analyzed by 15% native polyacrylamide gel electrophoresis and autoradiography.

generated a substrate that was extended by the polymerase to a complete 50-bp duplex molecule (Fig. 4). This confirms the result shown in Fig. 2B that Rad1-Rad10 removes the 3′ single-stranded tail, and indicates that Rad1-Rad10 cleavage products contain 3′-OH groups, the required substrate for extension by DNA polymerase. Hence, Rad1-Rad10 endonuclease products are suitable substrates for a necessary subsequent step in both the SSA recombination and NER models.

REFERENCES AND NOTES

1. E. C. Friedberg, W. Siede, A. J. Cooper, in *The Molecular and Cellular Biology of the Yeast* Saccharomyces: *Genome Dynamics, Protein Synthesis and Energetics*, J. Broach, E. Jones, J. Pringle, Eds. (Cold Spring Harbor Laboratory Press, Cold Spring Harbor, NY, 1991), pp. 147–192.
2. A. Aguilera and H. L. Klein, *Genetics* **123**, 683 (1989).
3. H. L. Klein, *ibid.* **120**, 367 (1988).
4. B. J. Thomas and R. Rothstein, *ibid.* **123**, 725 (1989).
5. B. R. Zehfus, A. D. McWilliams, Y. H. Lin, M. F. Hoekstra, R. L. Keil, *ibid.* **126**, 41 (1990).
6. R. H. Schiestl and S. Prakash, *Mol. Cell. Biol.* **8**, 3619 (1988).
7. ———, *ibid.* **10**, 2485 (1990).
8. J. Fishman-Lobell and J. E. Haber, *Science* **258**, 480 (1992).
9. A. M. Bailis, L. Arthur, R. Rothstein, *Mol. Cell. Biol.* **12**, 4988 (1992).
10. M. Biggerstaff, D. E. Szymkowski, R. D. Wood, *EMBO J.* **12**, 3685 (1993).
11. A. J. van Vuuren *et al.*, *ibid.*, p. 3693.
12. M. van Duin *et al.*, *Cell* **44**, 913 (1986).
13. A. J. Bardwell, L. Bardwell, D. K. Johnson, E. C. Friedberg, *Mol. Microbiol.* **8**, 1177 (1993).
14. L. Bardwell, A. J. Cooper, E. C. Friedberg, *Mol. Cell. Biol.* **12**, 3041 (1992).
15. A. E. Tomkinson, A. J. Bardwell, L. Bardwell, N. J. Tappe, E. C. Friedberg, *Nature* **362**, 860 (1993).
16. P. Sung, P. Reynolds, L. Prakash, S. Prakash, *J. Biol. Chem.* **268**, 26391 (1993).
17. A. J. Bardwell, L. Bardwell, A. E. Tomkinson, E. C. Friedberg, data not shown.
18. J.-C. Huang, D. L. Svoboda, J. T. Reardon, A. Sancar, *Proc. Natl. Acad. Sci. U.S.A.* **89**, 3664 (1992).
19. L. Bardwell *et al.*, *ibid.* **91**, 3926 (1994).
20. A. J. Bardwell *et al.*, *Mol. Cell. Biol.* **14**, 3569 (1994).
21. W. J. Feaver *et al.*, *Cell* **75**, 1379 (1993).
22. We have not detected exonuclease activity on single-stranded, double-stranded or 5′-tailed DNA oligonucleotides incubated with Rad1-Rad10, nor on phage DNA (*15*, *28*). However, we cannot formally exclude the possibility that the Rad1-Rad10 activity observed on the 3′-tailed and partial duplex structures in this study is a combined endonuclease-exonuclease with specificity for 3′ tails.
23. Y. Habraken, P. Sung, L. Prakash, S. Prakash, *Nature* **366**, 365 (1993).
24. J. J. Harrington and M. R. Lieber, *Genes Dev.* **8**, 1344 (1994).
25. Recent studies [A. O'Donovan, A. A. Davies, J. G. Moggs, S. C. West, R. D. Wood, *Nature*, in press] have shown that XPG protein (the human homolog of yeast Rad2 protein) is a junction-specific endonuclease that cuts DNA at duplex–5′ single-strand regions.
26. F. Lin, K. Sperle, N. Sternberg, *Mol. Cell. Biol.* **4**, 1020 (1984).
27. B. A. Ozenberger and G. S. Roeder, *ibid.* **11**, 1222 (1991).
28. A. E. Tomkinson, A. J. Bardwell, N. Tappe, W. Ramos, E. C. Friedberg, *Biochemistry* **33**, 5305 (1994).
29. Rad1 and Rad10 proteins were purified as described (*15*, *28*) [L. Bardwell, H. Burtscher, W. A. Weiss, C. M. Nicolet, E. C. Friedberg, *Biochemistry* **29**, 3119 (1990)]. Constituent oligonucleotides for each substrate (see Table 1) were mixed, heated to 95°C, and annealed by cooling to room temperature. Endonuclease reactions were carried out at 37°C for 40 min in 20-μl volumes containing 50 mM tris (pH 8.5), 5 mM $MgCl_2$, 5 mM dithiothreitol, and 1 pmol of substrate DNA. Reactions were stopped, deproteinized, and analyzed by gel electrophoresis and autoradiography. The low specific activity of Rad1-Rad10 enzyme has been previously observed (*15*, *16*).

30. We thank N. Tappe for assistance with protein purification. A.J.B. has previously published under the name A. J. Cooper. Supported by research grants CA12428 from the U.S. Public Health Service (E.C.F.) and grant 3786 from the Council for Tobacco Research (A.E.T.).

12 May 1994; accepted 17 August 1994

Padlock Probes: Circularizing Oligonucleotides for Localized DNA Detection

Mats Nilsson, Helena Malmgren, Martina Samiotaki, Marek Kwiatkowski, Bhanu P. Chowdhary, Ulf Landegren*

Nucleotide sequence information derived from DNA segments of the human and other genomes is accumulating rapidly. However, it frequently proves difficult to use such short DNA segments to identify clones in genomic libraries or fragments in blots of the whole genome or for in situ analysis of chromosomes. Oligonucleotide probes, consisting of two target-complementary segments, connected by a linker sequence, were designed. Upon recognition of the specific nucleic acid molecule the ends of the probes were joined through the action of a ligase, creating circular DNA molecules catenated to the target sequence. These probes thus provide highly specific detection with minimal background.

The application of synthetic oligonucleotides in combination with nucleic acid–specific enzymes has brought simplicity and convenience to molecular genetic analyses. There is, however, a need for methods in which oligonucleotides can be used for localized detection of single-copy gene sequences and for distinction among sequence variants in microscopic specimens. Such methods would help to bridge the analytic gap between specific gene sequences and subcellular structures. We have developed oligonucleotide probe molecules that should be useful for localized detection of specific nucleic acids. These "padlock" probes are composed of two target-complementary segments, connected by a linker that may carry detectable functions. The two ends of the linear oligonucleotide probes are brought in juxtaposition by hybridization to a target sequence. This juxtaposition allows the two probe segments to be covalently joined by the action of a DNA ligase. Because of the helical nature of DNA, circularized probes are wound around the target strand, topologically connecting probes to target molecules through catenation, in a manner similar to padlocks. The requirement for simultaneous hybridization of two different probe segments to target molecules provides for high specificity of detection in complex populations of nucleic acids (*1*). Moreover, the act of ligation permits facile distinction among similar target sequence variants as terminally mismatched probes are poor substrates for ligases (*1*, *2*). Finally, the covalent catenation of probe molecules to target sequences described here results in the formation of a hybrid that resists extreme washing conditions, serving to reduce nonspecific signals in genetic assays.

Probes useful for circularization experiments were constructed by solid phase synthesis of oligonucleotides that contained two hybridizing regions of 20 nucleotides each, connected by a 50-nucleotide-long linker segment (Fig. 1). Phosphate groups were added at the 5′ ends of the molecules as required for enzymatic ligation. Alternatively, residues of hexaethylene glycol (HEG) were incorporated in the linker segment during standard solid phase synthesis (*3*). The HEG residues served to reduce the number of synthetic steps required to span the ends of the two target-complementary segments.

Cyclizable probes were designed to detect a 40-nucleotide target sequence, represented either by an oligonucleotide molecule or by the polylinker sequence of the single-stranded form of the circular cloning vector M13 mp18. Ligation products could be separated by denaturing polyacrylamide gel electrophoresis (Fig. 2A). In the presence of the oligonucleotide target, linear probes were efficiently converted to circular molecules with a

M. Nilsson, H. Malmgren, M. Samiotaki, M. Kwiatkowski, U. Landegren, The Beijer Laboratory, Department of Medical Genetics, Box 589 Biomedical Center, S-75123 Uppsala, Sweden.
B. P. Chowdhary, Department of Animal Breeding and Genetics, Swedish University of Agricultural Sciences, Box 7023, S-750 07 Uppsala, Sweden.
*To whom correspondence should be addressed.